Multimodality imaging in metabolic heart disease

Ng, A.

6

Impact of Epicardial Adipose Tissue, Left Ventricular Myocardial Fat Content and Interstitial Fibrosis on Myocardial Contractile Function

Arnold C.T. Ng, Mark Strudwick, Rob J. van der Geest, Austin C.C. Ng, Lisa Gillinder, Shi Yi Goo, Gary Cowin, Victoria Delgado, William Y.S. Wang, Jeroen J. Bax

Circ Cardiovasc Imaging. 2018;11(8):e007372

ABSTRACT

Background: Current understanding of metabolic heart disease consists of myriad of different pathophysiological mechanisms. Epicardial adipose tissue (EAT) is increasingly recognized as metabolically active and associated with adverse cardiovascular outcomes. The present study aimed to investigate the effect of increased EAT volume index on left ventricular (LV) myocardial fat content (LV-myoFat) and burden of interstitial myocardial fibrosis, and their subsequent effects on LV myocardial contractile function.

Methods: 40 volunteers (mean age 35 ± 10 years, 26 males) of varying body mass index (BMI: 25.0 ± 4.1 kg/m^2, range 19.3–36.3 kg/m^2) and without diabetes or hypertension were prospectively recruited. EAT volume index, LV-myoFat and extracellular volume (ECV) were quantified by magnetic resonance imaging (MRI). LV myocardial contractile function was quantified by speckle tracking echocardiography global longitudinal strain (GLS) on the same day as MRI examination.

Results: Mean total EAT volume index, LV-myoFat and ECV were 30.0 ± 19.6 cm^3/m^2, 5.06 ± 1.18% and 27.5 ± 0.5% respectively. On multivariable analyses, increased EAT volume index and insulin resistance were independently associated with both increased LV-myoFat content and higher burden of interstitial myocardial fibrosis. Furthermore, increased EAT volume index was independently associated with LV GLS.

Conclusions: Increased EAT volume index and insulin resistance were independently associated with increased myocardial fat accumulation and interstitial myocardial fibrosis. Increased EAT volume index was associated with detrimental effects on myocardial contractile function as evidenced by a reduction in LV GLS.

INTRODUCTION

There is a growing body of evidence that the altered metabolic milieu seen in obese and diabetic patients causes myocardial structural changes and contractile dysfunction.[1] Commonly referred to as metabolic heart disease, we have previously shown that impaired left ventricular (LV) myocardial systolic function as quantified by 2-dimensional (2D) global longitudinal strain (GLS) echocardiography was associated with increased myocardial fat accumulation, coronary artery disease, increased interstitial fibrosis, and increased epicardial adipose tissue (EAT) volume.[2-5] EAT is depot of visceral fat directly overlying the myocardium, and is of similar embryological origin as abdominal mesenteric and omental visceral fat.[6] Increasingly, EAT is recognized as a metabolically active endocrine organ that secretes adipokines associated with detrimental myocardial and coronary vascular dysfunction.[7] Several studies have demonstrated a direct correlation between EAT and myocardial fat (i.e. triglyceride [TG]) accumulation,[8, 9] and animal research suggested that EAT may directly channel fatty acids to the myocardium as a local energy source.[10, 11] However, when the amount of free fatty acid uptake by the heart exceeds its oxidative capacity, it is converted and stored as intracellular TG.[12] It is currently accepted that the intracellular myocardial TG is probable inert, but increased shunting of free fatty acid into the non-oxidative pathway leads to accumulation of toxic fatty acid intermediates such as ceramide that disrupt normal cellular signaling and eventually leads to cellular apoptosis and replacement fibrosis.[13]

Magnetic resonance imaging (MRI) techniques such as proton magnetic resonance spectroscopy ([1H]-MRS) and multi-echo Dixon water and fat separated imaging with variable projection (VARPRO) can quantify LV myocardial fat (LV-myoFat) content.[14, 15] Similarly, the modified Look-Locker inversion recovery (MOLLI) sequence can quantify the burden of interstitial fibrosis by extracellular volume (ECV) expansion.[16, 17] In the present study, volunteers of normal weight, as well as overweight and obese individuals without the confounding influences of diabetes or hypertension were evaluated to determine the effect of increased EAT volume index on LV-myoFat content and burden of LV interstitial fibrosis. We hypothesize that: 1) increased EAT volume index is independently associated with increased myocardial fat accumulation and interstitial fibrosis; and 2) EAT volume index is independently associated with myocardial contractile function.

METHODS

Study population and study protocol

A total of 40 volunteers with a wide range of body mass index (BMI) were prospectively recruited from the community. Exclusion criteria included age < 18 years, pregnancy, rhythm other than sinus rhythm, hypertension, diabetes mellitus, previously known underlying coronary artery disease, LV systolic dysfunction or previous myocardial infarction, moderate or severe valvular stenosis or regurgitation, pre-existing hepatic or renal disorders, active smoker, current use of any regular medications, inability to provide informed consent, and inability to undergo a cardiac MRI. All participants' blood tests, transthoracic echocardiogram and cardiac MRI examinations were performed on the same day after an overnight fast.

Figure 1 outlines the study protocol. In brief, a subset of 15 randomly selected volunteers underwent "clinical reference standard" [1H]-MRS to validate LV-myoFat content by VARPRO. All 40 volunteers underwent cardiac MRI to quantify LV volumes, LV mass, EAT volume, LV-myoFat content by the VARPRO, and burden of LV interstitial fibrosis by ECV using the MOLLI sequence. [4, 16, 17] All 40 volunteers also underwent echocardiograms to quantify myocardial contractile function by 2D LV GLS.

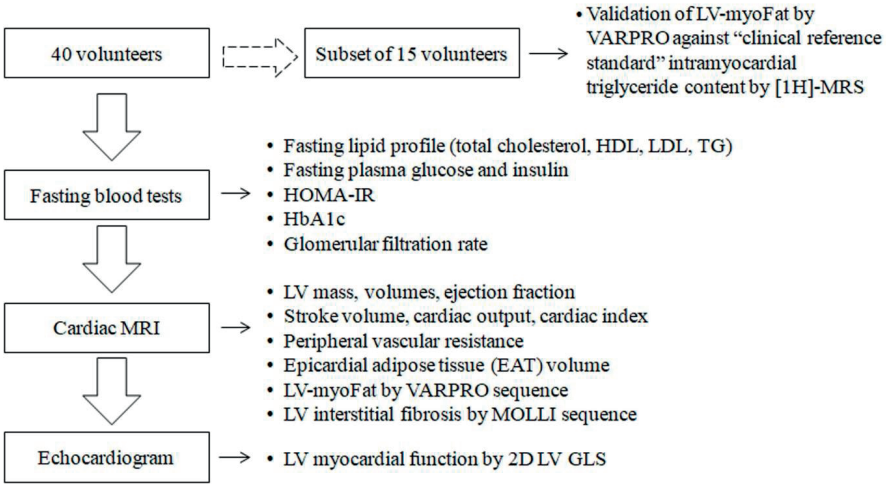

Figure 1. *Outline of study protocol. Subset of 15 volunteers underwent quantification of myocardial TG by [1H]-MRS to validate LV-myoFat by the VARPRO sequence. All 40 volunteers underwent fasting blood tests, cardiac MRI and echocardiography on the same day after an overnight fast. LV-myoFat = left ventricular myocardial fat; [1H]-MRS = proton magnetic resonance imaging; HDL = high density lipoprotein; LDL = low density lipoprotein; TG = triglyceride; HOMA-IR = homeostatic model assessment index of insulin resistance; HbA1c = glycated hemoglobin; VARPRO = variable projection; MOLLI = modified Look-Locker inversion recovery; LV = left ventricle/ventricular; 2D = 2-dimensional; GLS = global longitudinal strain.*

The study was approved by the institutional ethics committee and all subjects provided written informed consent. The data, analytic methods, and study materials will not be made available to other researchers for purposes of reproducing the results or replicating the procedure for competitive reasons.

Demographic, anthropomorphic and metabolic data

All subjects underwent an overnight fast of at least 8 hours. Clinical data collected included age, gender, height, weight, waist/hip ratio, and resting blood pressures. Waist circumference was measured midway between the lower rib margin and iliac crest. Hip circumference was measured at the level of widest circumference over greater trochanters.[18] Blood tests included fasting lipid profile, fasting plasma glucose, glycated hemoglobin (HbA1c), insulin, and glomerular filtration rates (GFR) calculated by the Modification of Diet in Renal Disease formula.[19]

High-density lipoprotein (HDL) cholesterol was measured as a homogeneous assay in liquid phase (Boehringer Mannheim, Mannheim, Germany) on a Hitachi 747 autoanalyzer. Low-density lipoprotein (LDL) cholesterol was calculated according to the Friedewald equation: LDL-cholesterol (mmol/L) = Total cholesterol – HDL-cholesterol – TG / 2.2.

Fasting plasma glucose was measured by enzymatic assay (Dade Behring, Newark, DE, USA). Serum insulin was evaluated using a chemiluminescent enzyme immunoassay (Immulite 2000; Diagnostic Products, Los Angeles, CA, USA). The homeostatic model assessment (HOMA) index of insulin resistance (HOMA-IR) was computed using the HOMA calculator that utilizes the HOMA2 model as previously reported.[20] HbA1c measurements were performed using high performance liquid chromatography cation-exchange analyzers by Bio-Rad D-10™ Hemoglobin Testing System (Bio-Rad Laboratories, Inc., Hercules, CA). This assay is National Glycohemoglobin Standardization Program (NGSP) and International Federation of Clinical Chemistry and Laboratory Medicine (IFCC) certified, and standardized to the Diabetes Control and Complications Trial (DCCT) assay.

Cardiac magnetic resonance imaging

All participants underwent a cardiac MRI examination using a 1.5T Siemens Magnetom Avanto (Erlangen, Germany) system on the same day as their transthoracic echocardiogram and blood tests. During the examination, the entire heart was imaged in the short-axis orientation with retrospective ECG-gating and breath-hold. Typical imaging parameters were: balanced steady state free-precession imaging, echo time (TE) = 1.0 ms, repetition time (TR) = 3.1 ms, flip angle = 54°, slice thickness = 8 mm with a gap of 2 mm, field of view = 340x340 mm, reconstructed matrix size = 156x192.

LV end-diastolic mass index, LV end-diastolic volume index (EDVI) and LV end-systolic volume index (ESVI) were measured and corrected for body surface area.[21] LV ejection fraction (LVEF) was calculated and expressed as a percentage. Differences in LV end-diastolic and end-systolic volumes were used to calculate stroke volume, multiplied by heart rate to calculate cardiac output, and corrected for body surface area to calculate cardiac index. Peripheral vascular resistance was calculated as the ratio of mean blood pressure to cardiac output. Images were digitally stored on hard disks and analyzed offline using dedicated quantitative software (MASS V2010-EXP, Leiden University Medical Center, Leiden, The Netherlands).

MRI quantification of myocardial triglyceride/fat content

Quantification of myocardial TG content by [1H]-MRS is considered the "clinical reference standard", but is time consuming to perform (mean scan duration 13.2 ± 4.5min).[13, 22] In contrast, newer MRI techniques such as VARPRO can rapidly obtain fat and water separated images to quantify LV-myoFat content in a single breath-hold. Furthermore, it can avoid contamination from EAT. Therefore, a subset of 15 volunteers underwent concomitant [1H]-MRS to validate LV-myoFat by VARPRO.

Quantification of myocardial triglyceride content by [1H]-MRS

Cardiac [1H]-MRS was performed as previously described (Figure 2, top panels).[2,22] Briefly, [1H]-MRS spectra were obtained by point resolved spectroscopy sequence (PRESS) with an 6mL voxel (1x2x3 cm) placed in the interventricular septum using the 4-chamber and short-axis views at end-diastole. Spectroscopic data acquisitions were double-triggered with ECG triggering and respiratory navigator echoes to minimize motion artifacts. End-diastolic spectra were acquired with the following parameters: TE = 25 ms, TR = 2000 ms, 1024 data points, bandwidth 1000Hz. Automatic shimming was performed before the spectroscopy data acquisition using the gradient-recalled echo shim technique whereby a field map was generated from a single-slab double-echo 3D gradient-recalled echo acquisition with two in-phase TEs with respect to fat and water, which were then used to calculate the shim currents to improve B0 homogeneity. Water-suppressed spectra were acquired with 128 signal averages to quantify myocardial TG. Non-water suppressed spectra were acquired with 16 signal averages and used as an internal standard.

[1H]-MRS data were then fitted by use of Java-based MR user interface software (jMRUI version 2.2, Leuven, Belgium) AMARES algorithm as previously described.[2] Resonance frequency estimates for myocardial TG were described by assuming Gaussian line shapes and summing the amplitudes of lipid resonances at 0.9 and 1.3 ppm. Resonance frequency estimate for water used for internal standardization was described by assuming a Lorentzian line shape that peaks at 4.7ppm. Myocardial TG content relative

to water was calculated and expressed as a percentage based on: (signal amplitude of myocardial TG)/(signal amplitude of water)x100%.[2]

Quantification of LV-myoFat content by VARPRO sequence

The VARPRO multi-point Dixon algorithm is a multi-echo gradient sequence with fat and water separation.[14, 23, 24] This multi-echo Dixon fat-water separation jointly estimates the fieldmap, fat, and water images (Figure 2, middle panel). The sequence was ECG triggered, with 2 R-R intervals between inversions, and used an echo-train readout with 4 echoes. Typical imaging parameters were: gradient echo, TE = 1.27, 3.18, 5.09, 7.00 ms, TR = 11.2 ms, flip angle = 24°, slice thickness 6 mm, field of view = 360 x 292 mm, reconstructed matrix size = 256x218, bandwidth = 1502 Hz/pixel. The LV basal and mid-ventricular short-axis slices by the VARPRO sequence were obtained at exactly the same LV level as quantification of interstitial fibrosis by MOLLI sequence (see below).

During analysis, the LV contours at the basal and mid-ventricular short axis slices were deliberately drawn in the mid-myocardium to exclude and avoid contamination by EAT and the LV blood pool using MASS research software. Although the LV apical segments were also acquired during the VARPRO image acquisitions, it was not included in the analyses due to partial volume effects from EAT and LV blood pool secondary to the curvature of the LV apex that will compromise accurate quantifications of LV-myoFat content. LV-myoFat fat content was calculated and expressed as a percentage based on: (mean pixel signal intensity of LV fat-only image)/(mean pixel signal intensity of LV water-only image)x100%.

MRI quantification of LV interstitial fibrosis by MOLLI sequence

The MOLLI T1 mapping sequence was used to quantify the burden of interstitial fibrosis by ECV.[16, 17] All participants received 0.1mmol/kg of gadolinium diethylenetriamine penta-acetic acid. The MOLLI sequence imaging parameters were: single-shot steady-state free precession read out with trigger delay to coincide with end-diastole, TE = 1.0 ms, TR = 2.7 ms, flip angle = 35°, slice thickness = 8mm, field of view = 340x340 mm, reconstructed matrix size = 106x192 pixels, trigger delay = 300ms. The LV basal and mid-ventricular short-axis slices by the MOLLI sequence were obtained at exactly the same LV level as quantification of LV-myoFat content by VARPRO. These images were then processed with a curve fitting technique to generate T1 maps as described below.

To quantify the ECV, LV endocardial and epicardial borders were outlined using MASS research software.[4, 25] Contours were deliberately drawn to ensure the inclusion of only myocardium and the exclusion of EAT and LV blood pool. The software then performs automatic pixel-by-pixel quantification of myocardial T1 time by fitting data acquired

at the various inversion times.[4, 25] A mean global native and post-contrast myocardial T1 time were subsequently automatically calculated as the average of all the individual myocardial T1 time from each pixel. ECV was calculated as per previous publication and expressed as a percentage [16]:

$$Myocardial\ ECV = (1 - haematocrit) \times \frac{\left(\frac{1}{post\ contrast\ myocardial\ T1} - \frac{1}{native\ myocardial\ T1}\right)}{\left(\frac{1}{post\ contrast\ blood\ T1} - \frac{1}{native\ blood\ T1}\right)}$$

A higher ECV is indicative of increased collagen deposition and thus a greater degree of myocardial interstitial fibrosis.

MRI quantification of epicardial adipose tissue volume

Total EAT volume was quantified using a T1 weighted double inversion recovery Half-Fourier-Acquired Single-shot Turbo spin Echo (HASTE) black blood imaging (Figure 2, bottom panels). Manual contours were drawn whereby mediastinal fat and pericardial fat (outside the visceral pericardium and on the external surface of the parietal pericardium) were excluded. The volumes of EAT in all the slices were calculated by converting the number of pixels to square centimetres multiplied by the slice thickness. Total EAT volume was subsequently calculated by summing the volumes of all slices from the level of pulmonary artery bifurcation to the diaphragm and indexed to body surface area. Typical imaging parameters were: turbo spin echo, TE = 26.0 ms, TR = 1000 ms depending on RR interval, flip angle = 160°, slice thickness 6 mm with a gap of 6 mm, field of view = 440x440 mm, reconstructed matrix size = 256x176.

MRI quantification of visceral adiposity

Abdominal visceral fat depots were quantified by using the VARPRO sequence with similar imaging parameters as outlined previously. Six consecutive transverse images were obtained with the middle image at the middle of the fourth lumbar vertebra. Similarly, manual contours were drawn to include only the abdominal visceral fat, and the volumes of the visceral fat depots in each slice was calculated by converting the number of pixels to square centimeters multiplied by the slice thickness. The total L4 visceral fat volume was calculated by summing the volumes of all 6 slices.

Echocardiography

Transthoracic echocardiography was performed with the subjects at rest using a commercially available ultrasound system (Vivid E9, 4V probe, GE-Vingmed, Horten, Norway) on the same day as their cardiac MRI and blood tests. A complete 2D, color, pulsed

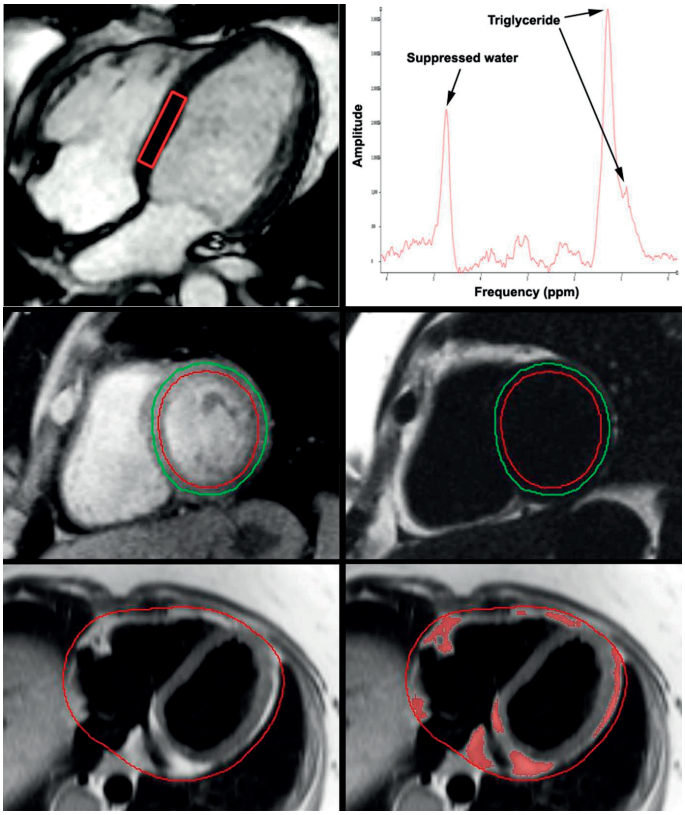

Figure 2. *Quantification of myocardial TG by "clinical reference standard" [1H]-MRS with the voxel of interest placed in the interventricular septum (top left panel). Myocardial TG was calculated from the summation of the lipid resonance amplitudes at 0.9 and 1.3ppm (top right panel). Quantification of LV-myoFat by VARPRO where epicardial and endocardial borders were deliberately drawn in the mid-myocardium to avoid contamination from EAT and LV blood pool (middle panels). The "water only" (middle left panel) and "fat only" (middle right panel) were obtained simultaneously from VARPRO, and both the endocardial and epicardial contours were identical on both images. Example of quantification of EAT volume (bottom panels).*

and continuous-wave Doppler echocardiogram was performed according to standard techniques.[26] All images were digitally stored on hard disks for offline analysis (EchoPAC version 113, GE-Vingmed, Horten, Norway).

Doppler assessment

Mitral inflow velocities were recorded using conventional pulsed-wave Doppler echocardiography in the apical 4-chamber view using a 2 mm sample volume. Transmitral early (E wave) and late (A wave) diastolic velocities as well as deceleration time were recorded at the mitral leaflet tips. Pulsed-wave tissue Doppler velocities were recorded at the septal mitral annulus in the apical 4-chamber view at end-expiration as recommended to obtain the mitral annular early diastolic (e') velocity.[27] LV filling pressure (septal E/e') was calculated as the ratio of transmitral E wave to septal mitral annular e' velocity.

Two-dimensional speckle tracking

2D speckle tracking analyses were performed on standard grey scale images in the apical 2-, 3- and 4-chamber views. During analysis, the endocardial border was manually traced at end-systole and the region of interest width adjusted to include the entire myocardium. LV GLS was calculated from the 3 individual apical global longitudinal strain curves.

Statistical analysis

All continuous variables were tested for Gaussian distribution. Continuous variables were presented as mean ±1 SD unless otherwise stated, and categorical variables were presented as frequencies and percentages. Unpaired Student's t-test and Mann-Whitney U test were used to compare 2 groups of continuous variables of Gaussian and non-Gaussian distribution respectively. Pearson correlation was used to determine the association between 2 continuous variables. Intraclass correlation and Bland-Altman plot were used to validate VARPRO to quantify LV-myoFat content against "clinical reference standard" myocardial TG content by [1H]-MRS. Multiple linear regression analyses were performed to identify independent variables associated with LV-myoFat content by VARPRO sequence, ECV as a measure of LV interstitial fibrosis, and 2D LV GLS by speckle tracking echocardiography. In each multiple linear regression model, significant univariables with $p < 0.05$ were entered as covariates and independent variables were identified using the backward elimination method. To avoid potential multicollinearity, a tolerance of > 0.4 (equating to a Variance Inflation Factor of > 2.5) was set. To determine if EAT volume index was independently associated with LV-myoFat, ECV, and 2D LV GLS (rather than just a measure of overall visceral adiposity), all multivariable analyses were repeated with L4 visceral fat volume forced into the models. A 2-tailed p value of < 0.05 was considered significant. All statistical analyses were performed using IBM SPSS Statistics for Windows, version 21.0 (Armonk, NY).

RESULTS

A total of 40 volunteers (26 males) with a mean age of 35 ± 10 years were recruited. The mean heart rate, LVEDVI, LVESVI, LVEF and LV mass index were 61 ± 9 beats/min, 90 ± 15 mL/m^2, 40 ± 8 mL/m^2, 55 ± 4% and 43 ± 8 g/m^2 respectively.

The mean BMI was 25.0 ± 4.1 kg/m^2 (range 19.3 to 36.3 kg/m^2), and the mean waist/hip ratio was 0.88 ± 0.11 (range 0.74 to 1.33). Twenty-two volunteers (55.0%) were identified as overweight/obese based on waist/hip ratio as classified by the World Health Organization cut-off values. The mean total EAT volume index was 30.0 ± 19.6 cm^3/m^2, and there was no gender difference in EAT volume index ($p = 0.28$).

Table 1. *Clinical, MRI and echocardiographic characteristics of study population.*

Variable	All Volunteers (n = 40)	Volunteers without [1H]-MRS (n = 25)	Volunteers with [1H]-MRS (n = 15)	p value*
Clinical				
Age (years)	35 ± 10	35 ± 11	36 ± 9	0.79
Male gender	26 (65%)	16 (64%)	10 (67%)	0.86
Waist/hip ratio	0.88 ± 0.11	0.88 ± 0.10	0.89 ± 0.14	0.92
Heart rate (beats/min)	61 ± 9	61 ± 10	60 ± 8	0.83
Systolic BP (mmHg)	128 ± 11	129 ± 11	126 ± 12	0.51
Diastolic BP (mmHg)	79 ± 9	79 ± 9	79 ± 10	0.97
Biochemical				
Total cholesterol (mmol/L)	4.82 ± 0.72	4.85 ± 0.72	4.78 ± 0.74	0.77
LDL cholesterol (mmol/L)	2.92 ± 0.56	2.93 ± 0.51	2.91 ± 0.66	0.89
HDL cholesterol (mmol/L)	1.44 ± 0.39	1.47 ± 0.47	1.40 ± 0.23	0.60
Plasma triglyceride (mmol/L)	1.03 ± 0.52	1.02 ± 0.48	1.04 ± 0.59	0.93
Fasting plasma glucose (mmol/L)	5.0 ± 0.5	5.0 ± 0.6	5.0 ± 0.3	0.67
HbA1c (%)	5.2 ± 0.2	5.2 ± 0.2	5.2 ± 0.3	0.93
Fasting Insulin (mU/L)	5.8 ± 5.1	6.2 ± 5.7	5.2 ± 4.1	0.99
HOMA-IR	1.30 ± 1.11	1.39 ± 1.24	1.16 ± 0.88	0.92
GFR (mL/min/1.73m^2)	99 ± 16	97 ± 17	101 ± 13	0.52
MRI				
LV mass index (g/m^2)	43 ± 8	43 ± 6	43 ± 10	0.89
LVEDVI (mL/m^2)	90 ± 15	91 ± 11	89 ± 21	0.74
LVESVI (mL/m^2)	40 ± 8	41 ± 6	39 ± 10	0.48
LVEF (%)	55 ± 4	55 ± 3	55 ± 4	0.58
Stroke volume (mL)	95 ± 19	95 ± 15	96 ± 25	0.81
Cardiac output (L/min)	5.7 ± 1.1	5.7 ± 1.1	5.7 ± 1.2	0.96
Cardiac index (L/min/m^2)	3.0 ± 0.6	3.0 ± 0.6	2.9 ± 0.6	0.80
Peripheral vascular resistance (dyn.s/cm^5)	1385 ± 288	1393 ± 318	1371 ± 240	0.82
L4 visceral fat volume (cm^3)	324 ± 239	227 ± 200	264 ± 219	0.60
EAT volume index (cm^3/m^2)	30.0 ± 19.6	27.3 ± 16.0	34.6 ± 24.3	0.26
LV-myoFat content (%)	5.1 ± 1.2	5.0 ± 1.1	5.2 ± 1.3	0.51
ECV (%)	27.5 ± 0.5	27.3 ± 0.5	27.8 ± 0.4	0.037
Echocardiography				
Transmitral E velocity (m/s)	0.77 ± 0.17	0.77 ± 0.18	0.78 ± 0.16	0.98
Transmitral E/A ratio	1.8 ± 0.8	1.8 ± 0.9	1.9 ± 0.6	0.77
Deceleration time (ms)	166 ± 28	169 ± 31	159 ± 20	0.26
Septal E' velocity (cm/s)	12.3 ± 3.0	11.9 ± 3.1	12.9 ± 2.6	0.30
Septal E/e' ratio	6.6 ± 1.8	6.8 ± 1.8	6.2 ± 1.8	0.33
2D LV GLS	-19.0 ± 2.4	-19.0 ± 2.7	-19.2 ± 2.0	0.77

*p value by unpaired Student's t-test or Mann-Whitney U test for continuous variables of Gaussian and non-Gaussian distribution respectively, and Chi square test for categorical variables. 2D: 2-dimensional; BP: blood pressure; EAT: epicardial adipose tissue; ECV: extracellular volume; EDVI: end-diastolic volume index; ESVI: end-systolic volume index; EF: ejection fraction; GFR: glomerular filtration rate; GLS: global longitudinal strain; HbA1c: glycated hemoglobin; HDL: high density lipoprotein; LDL: low density lipoprotein; HOMA-IR: homeostatic model assessment index of insulin resistance; LV: left ventricular; LV-myoFat: left ventricular myocardial fat content by VARPRO sequence.

Validation of VARPRO sequence against [1H]-MRS

A subset of 15 randomly volunteers underwent "clinical reference standard" [1H]-MRS to quantify myocardial TG content. Table 1 outlines the baseline clinical, MRI and echocardiographic characteristics between the 15 randomly selected volunteers against the rest of the cohort. Other than a slight difference in ECV between these 2 groups (27.3 ± 0.5 vs. 27.8 ± 0.4%, p = 0.037), there were no significant differences in other variables. Figures 3 and 4 show LV-myoFat content by VARPRO overestimated myocardial TG content compared to [1H]-MRS:

$$\textit{LV-myoFat content by VARPRO} = 1.31 \times (\textit{Intramyocardial TG by } [1H]\text{-}MRS) + 3.84$$

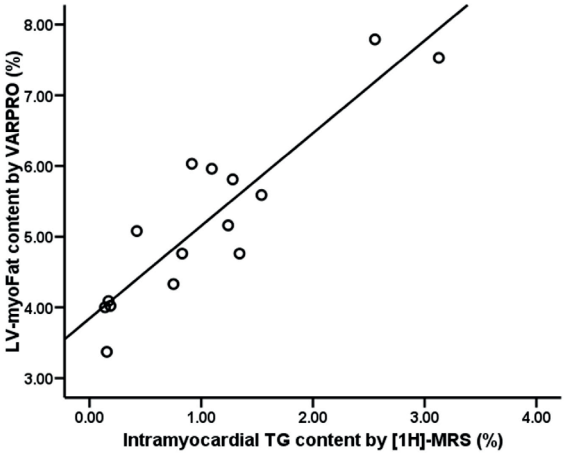

Figure 3. *Scatterplot showing excellent reliability of VARPRO quantification of LV-myoFat against "clinical reference standard" quantification of myocardial TG content by [1H]-MRS.*

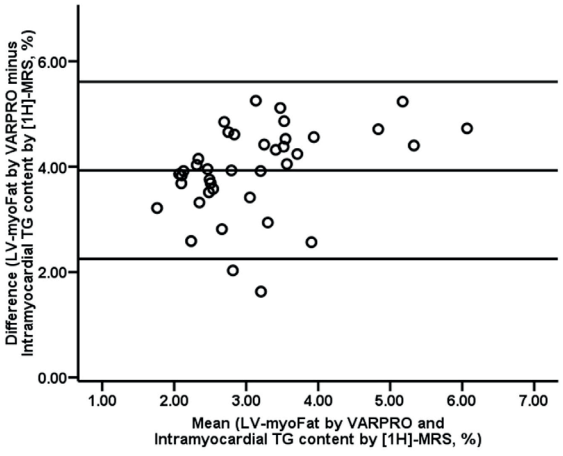

Figure 4. *Bland-Altman plot showing overestimation of VARPRO quantification of LV-myoFat against "clinical reference standard" quantification of myocardial TG content by [1H]-MRS.*

However, LV-myoFat content quantification by VARPRO had excellent reliability compared to the "clinical reference standard" myocardial TG quantification by [1H]-MRS with an intraclass correlation for consistency of r = 0.92 (95% confidence interval 0.75-0.97).

Determinants of LV-myoFat content

The mean LV-myoFat content by VARPRO for all 40 volunteers was 5.06 ± 1.18%. There was no gender difference in LV-myoFat content (p = 0.36). LV-myoFat content increased with older age (r = 0.51, p = 0.001), higher insulin resistance (HOMA-IR, r = 0.51, p = 0.001) and increasing measures of obesity by EAT volume index (r = 0.61, p < 0.001), waist/hip ratio (r = 0.59, p < 0.001) and L4 visceral fat volume (r = 0.60, p < 0.001). There was also a correlation between LV-myoFat content and plasma TG (r = 0.48, p = 0.002), LDL-cholesterol (r = 0.33, p = 0.038) and HDL-cholesterol (r = -0.37, p = 0.018), but not total cholesterol (p = 0.23).

To identify the independent variables associated with LV-myoFat content, significant univariables (age, HOMA-IR, EAT volume index, waist/hip ratio, plasma TG, LDL-cholesterol and HDL-cholesterol) were entered as covariates into a multiple linear regression model. On multivariable analysis, only HOMA-IR (standardized β = 0.32, p = 0.024) and EAT volume index (standardized β = 0.47, p = 0.002) were independently associated with LV-myoFat content.

To determine if increased EAT volume index was truly independently associated with LV-myoFat content rather than just a measure of overall visceral adiposity, waist/hip ratio was replaced with L4 visceral fat volume in the multiple linear regression model. Although L4 visceral fat volume was highly correlated with EAT volume index (r = 0.69, p < 0.001), it was forced into the multivariable model. Despite that, similar results were obtained with only HOMA-IR (standardized β = 0.32, p = 0.024) and EAT volume index (standardized β = 0.47, p = 0.002) remaining as significantly associated with LV-myoFat content.

Determinants of burden of LV interstitial fibrosis

The mean ECV was 27.5 ± 0.5%, and there was no gender difference (p = 0.88). On univariable analysis, ECV was significantly correlated with higher LV-myoFat content (r = 0.71, p < 0.001), older age (r = 0.64, p = 0.002), higher HOMA-IR (r = 0.51, p = 0.021) and increasing EAT volume index (r = 0.69, p = 0.001).

To identify the independent variables associated with ECV, significant univariables (age, LV-myoFat, HOMA-IR and EAT volume index) were entered as covariates into a multiple linear regression model. EAT volume index (standardized β = 0.46, p = 0.025)

and LV-myoFat content (standardized β = 0.41, p = 0.045) were independently associated with ECV. The results did not change when L4 visceral fat volume was forced into the multivariable model.

Determinants of LV myocardial function

The mean 2D LV GLS was -19.0 ± 2.4%, and women had significantly higher GLS than men (-20.3 ± 2.2 vs. -18.4 ± 2.3%, p = 0.013). 2D LV GLS was significantly correlated with age (r = 0.44, p = 0.005), HOMA-IR (r = 0.60, p < 0.001), EAT volume index (r = 0.66, p < 0.001), LV-myoFat (r = 0.50, p < 0.001) and ECV (r = 0.70, p < 0.001).

On multivariable analysis whereby age, gender, HOMA-IR, EAT volume index, LV-myoFat and ECV were entered into the model, only EAT volume index was independently associated with 2D LV GLS (standardized β = 0.44, p = 0.041). Similarly, when L4 visceral fat volume was forced into the model, only EAT volume index remained independently associated with 2D LV GLS.

Variability analysis

We have previously reported the intra- and inter-observer measurement variabilities for LV GLS expressed as mean absolute difference ± 1 SD were 1.2 ± 0.5% and 0.9 ± 1.0% respectively.[28] Table 2 outlines the intra- and inter-observer measurement variabilities for ECV, LV-myoFat content and EAT volume index expressed as mean absolute differences ± 1 SD and intraclass correlation for agreement in 10 randomly selected subjects.

Table 2. *Intra-observer and inter-observer measurement variability*

Variable	Intra-observer		Inter-observer	
	Absolute difference	ICC (95% CI)	Absolute difference	ICC (95% CI)
ECV	0.21 ± 0.08	0.97 (0.80 – 0.99)	0.28 ± 0.13	0.93 (0.73 – 0.98)
LV-myoFat	0.26 ± 0.19	0.98 (0.91 – 0.99)	0.42 ± 0.50	0.91 (0.67 – 0.98)
EAT volume index	3.0 ± 1.5	0.99 (0.96 – 0.99)	3.6 ± 2.2	0.99 (0.95 – 0.99)

CI: Confidence interval; EAT: Epicardial adipose tissue; ECV: Extracellular volume; ICC: Intraclass correlation; LV-myoFat: left ventricular myocardial fat content by VARPRO sequence.

DISCUSSION

The present study evaluated the complex interplay between insulin resistance, increased EAT volume, myocardial fat accumulation and LV interstitial fibrosis, leading to LV myocardial systolic dysfunction in volunteers with normal weight, as well as over-

weight and obese individuals. This study showed that insulin resistance and EAT volume index were independently associated with increased myocardial fat accumulation and LV interstitial fibrosis. On multivariable analyses, EAT volume index was independently associated with impaired LV myocardial systolic contractile function.

Quantification of LV-myoFat by VARPRO versus [1H]-MRS

In the present study, VARPRO significantly overestimated LV-myoFat content compared to [1H]-MRS. This is likely secondary to its inherent T1 bias, especially with its high flip angle. As previously shown by Kühn et al and Liu et al, increasing flip angle (≥5-10°) will overestimate fat fraction by chemical shift imaging compared to [1H]-MRS.[29, 30] However, a lower flip angle will significantly reduce the signal-to-noise ratio, and the noise can lead to incorrect estimation of the true fat fraction.[30] Although VARPRO significantly overestimated LV-myoFat content, it still had excellent correlation and reliability when compared to [1H]-MRS (Figure 3).

However, VARPRO has significant advantages over [1H]-MRS. Firstly, it permits regional and global LV quantification of LV-myoFat, whereas [1H]-MRS is limited to the interventricular septum due to the risk of contamination from EAT. Secondly, VARPRO is performed with a single breath-hold, whereas [1H]-MRS will require double respiratory and cardiac gating that will significantly increase scan duration.[22] Finally, slice positioning for various imaging sequences (e.g. VARPRO for LV-myoFat and MOLLI for interstitial fibrosis) can be consistently and completely matched as demonstrated in the present study.

Epicardial adipose tissue, insulin resistance and myocardial steatosis

The myocardium has a very high energy demand in order to perform cardiac contraction and relaxation. Under normal physiological conditions, it predominately metabolizes free fatty acids through β-oxidation which accounts for approximately 50-70% of its energy production.[7] Although the source of this free fatty acid is generally derived from circulating plasma triglyceride and free fatty acid, it is now recognized that EAT is a readily available local store of TG that directly release free fatty acid to the myocardium at times of increased cardiac fatty acid metabolism.[10, 11, 31] As such, the present study demonstrated that both increased EAT volume index and insulin resistance were independently associated with increased myocardial fat accumulation. This is consistent with previous studies that showed increased EAT volume in obese patients was associated with increased myocardial fat accumulation.[8, 9] In addition, type 2 diabetes, the archetypal disease where pathophysiology is characterized by insulin resistance, is also associated with increased myocardial fat accumulation.[2]

Epicardial adipose tissue and myocardial interstitial fibrosis

However, EAT is also now increasingly recognized as an endocrine organ that secretes adipokines.[7] Both EAT and the underlying myocardium share the same coronary microcirculation with no anatomical fascial boundary separating the 2 structures. As such, adipokines and cytokines secreted by EAT have a direct vasocrine and paracrine effect on coronary and myocardial function.[32] Secretions of pro-inflammatory adipokines such as IL-6, MCP-1, leptin and visfatin are increased with larger EAT volumes, while the secretions of anti-inflammatory adipokines such as adiponectin and adrenomedullin are decreased, all leading to increased coronary vasoconstriction, inflammation and atherosclerosis.[7] Furthermore, increased secretion of TNF-α from EAT has also been shown to induce cardiomyocyte apoptosis leading to replacement fibrosis.[33] Mazurek and colleagues previously demonstrated higher levels of pro-inflammatory cytokines such as IL-6 and TNF-α in EAT harvested from patients undergoing coronary artery bypass grafting compared to subcutaneous adipose tissue.[33] TNF-α worsens insulin resistance and causes vasoconstriction, which is also associated with increased production of angiotensin II and endothelin-1.[34, 35]

Previous studies have shown increased TNF-α is associated with cardiac dilatation, increased interstitial inflammatory infiltrates, abnormal calcium homeostasis, increased apoptosis, extracellular matrix remodeling, ventricular arrhythmias and death.[36, 37] To the best of the authors' knowledge, the present in-vivo study is the first to demonstrate larger EAT volumes is associated with increased myocardial interstitial fibrosis in humans.

Epicardial adipose tissue and myocardial contractility

In-vitro studies of EAT derived from guinea pigs fed a high fat diet [38] and diabetic patients undergoing coronary bypass surgery [39] showed that unlike subcutaneous adipose tissue, EAT have altered secretory profiles that directly contribute to cardiomyocyte contractile dysfunction. Mediated through adipokines including activin A and angiopoietin-2, they adversely affect cytosolic Ca^{2+} metabolism and reduce sarcomere shortening in a dose dependent manner.[38, 39] We have previously shown increased EAT volume was associated with myocardial systolic contractile dysfunction.[5] The present study extends these findings by showing that the observed myocardial contractile dysfunction often seen in obese and diabetic patients is likely secondary to functional (i.e. direct cardio-depressant effects of adipokines) and structural changes (i.e. increased myocardial interstitial fibrosis from inflammation secondary to adipokines) in the myocardium mediated by an increased EAT volume.

Clinical implications

The present findings suggest that EAT is a marker of visceral adiposity with direct adverse effects on myocardial structure and function. Therefore, it may be a target for pharmacological therapy and serve as a prognostic indicator. Previous small studies using hydroxymethyl glutaryl-CoAreductase inhibitors (i.e. statins) [40], dipeptidyl peptidase 4 inhibitors (e.g. sitagliptin) [41] and glucagon-like peptide-1 (e.g. liraglutide) [42] have been shown to reduce EAT volume. The effects of EAT volume reduction on myocardial structural and functional changes need to be assessed in future studies.

Study limitations

While the present study provides new and novel findings on myocardial structural and functional changes associated with EAT, the study only recruited volunteers of varying BMI but without diabetes or hypertension. This was to avoid potential confounding influences of diabetes and hypertension on myocardial interstitial fibrosis and altered myocardial contractile function. Therefore, the present results serve as a pilot for future studies in diabetic patients. Secondly, although the present study demonstrated significant independent associations between increased EAT volume index, increased LV-myoFat, increased interstitial fibrosis and LV myocardial contractile dysfunction, it does not equate to causality in humans despite various published in-vitro basic science as well as animal studies.

CONCLUSIONS

The current findings demonstrate that increased EAT was associated with LV myocardial fat accumulation and increased interstitial fibrosis. Both increased EAT and increased interstitial fibrosis were independently associated with myocardial contractile function. Therefore, therapeutic interventions targeting EAT may serve to modulate the detrimental effects of metabolic heart disease.

REFERENCE LIST

(1) Horwich TB, Fonarow GC. Glucose, Obesity, Metabolic Syndrome, and Diabetes: Relevance to Incidence of Heart Failure. *J Am Coll Cardiol* 2010;55(4):283-293.

(2) Ng AC, Delgado V, Bertini M, van der Meer RW, Rijzewijk LJ, Hooi ES, Siebelink HM, Smit JW, Diamant M, Romijn JA, de RA, Leung DY, Lamb HJ, Bax JJ. Myocardial steatosis and biventricular strain and strain rate imaging in patients with type 2 diabetes mellitus. *Circulation* 2010;122(24):2538-2544.

(3) Nucifora G, Schuijf JD, Delgado V, Bertini M, Scholte AJ, Ng AC, van Werkhoven JM, Jukema JW, Holman E, Van Der Wall E, Bax JJ. Incremental value of subclinical left ventricular systolic dysfunction for the identification of patients with obstructive coronary artery disease. *Am Heart J* 2010;159(1):148-157.

(4) Ng AC, Auger D, Delgado V, van Elderen SG, Bertini M, Siebelink HM, van der Geest RJ, Bonetti C, van der Velde ET, De Roos A, Smit JW, Leung DY, Bax JJ, Lamb HJ. Association between diffuse myocardial fibrosis by cardiac magnetic resonance contrast-enhanced T1 mapping and subclinical myocardial dysfunction in diabetic patients: a pilot study. *Circ Cardiovasc Imaging* 2012;5(1):51-59.

(5) Ng AC, Goo SY, Roche N, van der Geest RJ, Wang WY. Epicardial Adipose Tissue Volume and Left Ventricular Myocardial Function Using 3-Dimensional Speckle Tracking Echocardiography. *Can J Cardiol* 2016;32(12):1485-1492.

(6) Sacks HS, Fain JN. Human epicardial adipose tissue: a review. *Am Heart J* 2007;153(6):907-917.

(7) Patel VB, Shah S, Verma S, Oudit GY. Epicardial adipose tissue as a metabolic transducer: role in heart failure and coronary artery disease. *Heart Fail Rev* 2017;22(3):889-902.

(8) Kankaanpaa M, Lehto HR, Parkka JP, Komu M, Viljanen A, Ferrannini E, Knuuti J, Nuutila P, Parkkola R, Iozzo P. Myocardial triglyceride content and epicardial fat mass in human obesity: relationship to left ventricular function and serum free fatty acid levels. *J Clin Endocrinol Metab* 2006;91(11):4689-4695.

(9) Malavazos AE, Di LG, Secchi F, Lupo EN, Dogliotti G, Coman C, Morricone L, Corsi MM, Sardanelli F, Iacobellis G. Relation of echocardiographic epicardial fat thickness and myocardial fat. *Am J Cardiol* 2010;105(12):1831-1835.

(10) Marchington JM, Pond CM. Site-specific properties of pericardial and epicardial adipose tissue: the effects of insulin and high-fat feeding on lipogenesis and the incorporation of fatty acids in vitro. *Int J Obes* 1990;14(12):1013-1022.

(11) Nelson RH, Prasad A, Lerman A, Miles JM. Myocardial uptake of circulating triglycerides in nondiabetic patients with heart disease. *Diabetes* 2007;56(2):527-530.

(12) McGavock JM, Victor RG, Unger RH, Szczepaniak LS. Adiposity of the Heart, Revisited. *Ann Intern Med* 2006;144(7):517-524.

(13) Ng AC, Delgado V, Djaberi R, Schuijf JD, Boogers MJ, Auger D, Bertini M, De Roos A, van der Meer RW, Lamb HJ, Bax JJ. Multimodality imaging in diabetic heart disease. *Curr Probl Cardiol* 2011;36(1):9-47.

(14) Kellman P, Hernando D, Shah S, Zuehlsdorff S, Jerecic R, Mancini C, Liang ZP, Arai AE. Multiecho dixon fat and water separation method for detecting fibrofatty infiltration in the myocardium. *Magn Reson Med* 2009;61(1):215-221.

(15) Hernando D, Kellman P, Haldar JP, Liang ZP. Robust water/fat separation in the presence of large field inhomogeneities using a graph cut algorithm. *Magn Reson Med* 2010;63(1):79-90.

(16) Schelbert EB, Testa SM, Meier CG, Ceyrolles WJ, Levenson JE, Blair AJ, Kellman P, Jones BL, Ludwig DR, Schwartzman D, Shroff SG, Wong TC. Myocardial extravascular extracellular volume fraction measurement by gadolinium cardiovascular magnetic resonance in humans: slow infusion versus bolus. *J Cardiovasc Magn Reson* 2011;13:16.

(17) Messroghli DR, Greiser A, Frohlich M, Dietz R, Schulz-Menger J. Optimization and validation of a fully-integrated pulse sequence for modified look-locker inversion-recovery (MOLLI) T1 mapping of the heart. *J Magn Reson Imaging* 2007;26(4):1081-1086.

(18) World Health Organization. Waist circumference and waist-hip ratio: report of a WHO expert consultation. Geneva, 8-11 December 2008. Geneva, Switzerland: WHO. 2011.

(19) K/DOQI clinical practice guidelines for chronic kidney disease: evaluation, classification and stratification. *Am J Kidney Dis* 2002;39:S1-S266.

(20) Wallace TM, Levy JC, Matthews DR. Use and abuse of HOMA modeling. *Diabetes Care* 2004;27(6):1487-1495.

(21) Mosteller RD. Simplified calculation of body-surface area. *N Engl J Med* 1987;317(17):1098.

(22) Gillinder L, Goo SY, Cowin G, Strudwick M, van der Geest RJ, Wang WY, Ng AC. Quantification of Intramyocardial Metabolites by Proton Magnetic Resonance Spectroscopy. *Front Cardiovasc Med* 2015;2:24.

(23) Hernando D, Haldar JP, Sutton BP, Ma J, Kellman P, Liang ZP. Joint estimation of water/fat images and field inhomogeneity map. *Magn Reson Med* 2008;59(3):571-580.

(24) Kellman P, Hernando D, Arai AE. Myocardial Fat Imaging. *Curr Cardiovasc Imaging Rep* 2010;3(2):83-91.

(25) Gai N, Turkbey EB, Nazarian S, van der Geest RJ, Liu CY, Lima JA, Bluemke DA. T1 mapping of the gadolinium-enhanced myocardium: adjustment for factors affecting interpatient comparison. *Magn Reson Med* 2011;65(5):1407-1415.

(26) Lang RM, Badano LP, Mor-Avi V, Afilalo J, Armstrong A, Ernande L, Flachskampf FA, Foster E, Goldstein SA, Kuznetsova T, Lancellotti P, Muraru D, Picard MH, Rietzschel ER, Rudski L, Spencer KT, Tsang W, Voigt JU. Recommendations for cardiac chamber quantification by echocardiography in adults: an update from the American Society of Echocardiography and the European Association of Cardiovascular Imaging. *Eur Heart J Cardiovasc Imaging* 2015;16(3):233-270.

(27) Nagueh SF, Smiseth OA, Appleton CP, Byrd BF, III, Dokainish H, Edvardsen T, Flachskampf FA, Gillebert TC, Klein AL, Lancellotti P, Marino P, Oh JK, Popescu BA, Waggoner AD. Recommendations for the Evaluation of Left Ventricular Diastolic Function by Echocardiography: An Update from the American Society of Echocardiography and the European Association of Cardiovascular Imaging. *J Am Soc Echocardiogr* 2016;29(4):277-314.

(28) Ng ACT, Delgado V, Bertini M, van der Meer RW, Rijzewijk LJ, Shanks M, Nucifora G, Smit JWA, Diamant M, Romijn JA, De Roos A, Leung DY, Lamb HJ, Bax JJ. Findings from left ventricular strain and strain rate imaging in asymptomatic patients with type 2 diabetes mellitus. *Am J Cardiol* 2009;104(10):1398-1401.

(29) Kuhn JP, Jahn C, Hernando D, Siegmund W, Hadlich S, Mayerle J, Pfannmoller J, Langner S, Reeder S. T1 bias in chemical shift-encoded liver fat-fraction: role of the flip angle. *J Magn Reson Imaging* 2014;40(4):875-883.

(30) Liu CY, McKenzie CA, Yu H, Brittain JH, Reeder SB. Fat quantification with IDEAL gradient echo imaging: correction of bias from T(1) and noise. *Magn Reson Med* 2007;58(2):354-364.

(31) Stanley WC, Recchia FA, Lopaschuk GD. Myocardial substrate metabolism in the normal and failing heart. *Physiol Rev* 2005;85(3):1093-1129.

(32) Cherian S, Lopaschuk GD, Carvalho E. Cellular cross-talk between epicardial adipose tissue and myocardium in relation to the pathogenesis of cardiovascular disease. *Am J Physiol Endocrinol Metab* 2012;303(8):E937-E949.

(33) Mazurek T, Zhang L, Zalewski A, Mannion JD, Diehl JT, Arafat H, Sarov-Blat L, O'Brien S, Keiper EA, Johnson AG, Martin J, Goldstein BJ, Shi Y. Human epicardial adipose tissue is a source of inflammatory mediators. *Circulation* 2003;108(20):2460-2466.

(34) Zhang H, Park Y, Wu J, Chen X, Lee S, Yang J, Dellsperger KC, Zhang C. Role of TNF-alpha in vascular dysfunction. *Clin Sci (Lond)* 2009;116(3):219-230.

(35) Salazar J, Luzardo E, Mejias JC, Rojas J, Ferreira A, Rivas-Rios JR, Bermudez V. Epicardial Fat: Physiological, Pathological, and Therapeutic Implications. *Cardiol Res Pract* 2016;2016:1291537.

(36) Higuchi Y, McTiernan CF, Frye CB, McGowan BS, Chan TO, Feldman AM. Tumor necrosis factor receptors 1 and 2 differentially regulate survival, cardiac dysfunction, and remodeling in transgenic mice with tumor necrosis factor-alpha-induced cardiomyopathy. *Circulation* 2004;109(15):1892-1897.

(37) Sinagra E, Perricone G, Romano C, Cottone M. Heart failure and anti tumor necrosis factor-alpha in systemic chronic inflammatory diseases. *Eur J Intern Med* 2013;24(5):385-392.

(38) Greulich S, de Wiza DH, Preilowski S, Ding Z, Mueller H, Langin D, Jaquet K, Ouwens DM, Eckel J. Secretory products of guinea pig epicardial fat induce insulin resistance and impair primary adult rat cardiomyocyte function. *J Cell Mol Med* 2011;15(11):2399-2410.

(39) Greulich S, Maxhera B, Vandenplas G, de Wiza DH, Smiris K, Mueller H, Heinrichs J, Blumensatt M, Cuvelier C, Akhyari P, Ruige JB, Ouwens DM, Eckel J. Secretory products from epicardial adipose tissue of patients with type 2 diabetes mellitus induce cardiomyocyte dysfunction. *Circulation* 2012;126(19):2324-2334.

(40) Park JH, Park YS, Kim YJ, Lee IS, Kim JH, Lee JH, Choi SW, Jeong JO, Seong IW. Effects of statins on the epicardial fat thickness in patients with coronary artery stenosis underwent percutaneous coronary intervention: comparison of atorvastatin with simvastatin/ezetimibe. *J Cardiovasc Ultrasound* 2010;18(4):121-126.

(41) Lima-Martinez MM, Paoli M, Rodney M, Balladares N, Contreras M, D'Marco L, Iacobellis G. Effect of sitagliptin on epicardial fat thickness in subjects with type 2 diabetes and obesity: a pilot study. *Endocrine* 2016;51(3):448-455.

(42) Iacobellis G, Mohseni M, Bianco SD, Banga PK. Liraglutide causes large and rapid epicardial fat reduction. *Obesity (Silver Spring)* 2017;25(2):311-316.